30th Annual International IEEE EMBS Conference
Vancouver, British Columbia, Canada, August 20-24, 2008

Improvement of Automated Detection Method of Hemorrhages in Fundus Images

Yuji Hatanaka, Toshiaki Nakagawa, Yoshinori Hayashi, Takeshi Hara and Hiroshi Fujita

Abstract—**This paper describe an improved method for detecting hemorrhages in fundus images. The detection of hemorrhages is one of the important factors in the early diagnosis of diabetic retinopathy. So, we had suggested several methods for detecting abnormalities in fundus images, but our methods had some problems. We propose a new method for preprocessing and false positive elimination in the present study. The brightness of the fundus image was changed by the nonlinear curve with brightness values of the hue saturation value (HSV) space. In order to emphasize brown regions, gamma correction was performed on each red, green, and blue-bit image. Subsequently, the histograms of each red, blue, and blue-bit image were extended. After that, the hemorrhage candidates were detected using density analysis. Finally, false positives were removed by using rule-based method and 3 Mahalanobis distance classifiers with a 45-feature analysis. To evaluate the new method for the detection of hemorrhages, we examined 125 fundus images, including 35 images with hemorrhages and 90 normal images. The sensitivity and specificity for the detection of abnormal cases were 80% and 80%, respectively.**

I. Introduction

In Japan, there are approximately 7.4 million patients with diabetes and approximately 16.2 million patients who may have diabetes [1]. Approximately three million are thought to suffer from diabetic retinopathy (DR). This disease can be prevented from developing into blindness if it is treated at an early stage. However, it has been recorded that approximately 3,000 people have lost their vision following the onset of DR. Fundus photographs obtained by the fundus camera are used to diagnose DR. Japanese ophthalmologists usually examine the presence of hemorrhages, microaneurysms, and exudates in order to diagnose DR. By using fluorescein angiograms, the ophthalmologists could detect the hemorrhages and microaneurysms. However, it is difficult to use fluorescein as a contrast medium for diagnosing all the medical examinees subjected to mass screening. Therefore, the patients who show the possibility of having DR were thoroughly examined in a hospital.

Recently, many studies have been reported on the use of fundus images in the detection of DR [2–7]. Fleming et al. proposed a method for the detection of microaneurysms by using a watershed transform in fluorescein angiograms [2]. Serrano et al. proposed a method for detecting microaneurysms by the region growing technique in order to analyze fluorescein angiograms [3]. Usher et al. presented a method for detecting hemorrhages, microaneurysms, and exudates [4]. Niemeijer et al. proposed a method for the detection of red regions [5]. The sensitivity of their method was 100% and the specificity was 87%. The region growing method used by them segmented the abnormal and retinal regions. Moreover, the previous method had the drawback of a long computation time of approximately 15 minutes per image. Nagayoshi et al. presented a method that included the normalization processes to Usher's method [4]. Moreover, the previous method had the drawback of a long computation time of approximately 43 s per image [6]. Grisan et al. proposed a method for detecting the dark lesion based on local thresholding and pixel density [7]. They reported a mean detection rate of 94% of the lesions present in an image based on a dataset of 60 annotated images.

We have been attempting to develop a synthetic fundus CAD system [8-13]. We reported methods of detecting abnormal blood vessels to help in the diagnosis of hypertensive retinopathy [8, 9]. Moreover, we proposed a method of detecting retinal nerve fiber layer defects (NFLD) [10] and a method of calculating the cup to disc ratio (C/D ratio) [11] to help in the diagnosis of glaucoma. In addition, we proposed a technique to obtain the depth value from the stereo image pair of a retinal fundus for the 3-D reconstruction of the optic nerve head [12]. Further more, we also reported a method for detecting hemorrhages and exudates in noncontrast fundus images [13]. Although the sensitivity for hemorrhages was 85%, the specificity was 21%. In our previous study, we had two problems—the absence of a technique to normalize fundus images and the removal of false positives (FPs). In this study, we aim to develop methods for fundus image normalization and FPs elimination method in the noncontrast images.

Manuscript received April 7, 2008; revised July 3, 2008. This work was supported in part by a "Knowledge-Based Clusters" from the Ministry of Education, Culture, Sports, Science & Technology, Japan. The authors thank T. Yamamoto, K. Kawase, A. Sawada, S. Takimoto, Y. Mizukusa, T. Suzuki, M. Kakogawa, K. Sugio, H. Nonogaki and G. Lee for their significant contributions to this study.

Y. Hatanaka is with the Department of Electronic Systems Engineering, School of Engineering, University of Shiga Prefecture, Hassaka-cho 2500, Hikone-shi, Shiga 522-8533, Japan. (corresponding author to provide phone: 81-749-28-9556; e-mail: hatanaka.y@usp.ac.jp).

T. Nakagawa is with the Kowa Company Ltd., Chofugaoka 3-3-1, Chofu-shi, Tokyo 182-0021, Japan.

Y. Hayashi is with the TAK Co. Ltd., Kono 4-35-12, Ogaki 503-0803, Japan.

T. Hara and H. Fujita are with the Department of Intelligent Image Information, Graduate School of Medicine, Gifu University, Yanagido 1-1, Gifu 501-1194, Japan.

II. METHODS

A. Overall Scheme

Our overall detection scheme consists of six stages: (1) image digitization, (2) image normalization, (3) extraction of optic nerve head, (4) detection of hemorrhage candidates, (5) elimination of FPs in blood vessels, and (6) elimination of FPs by feature analysis. Further details are described below.

B. Image digitization

One hundred forty five fundus images were captured using a fundus camera and a flatbed-type scanner. Eighty seven fundus images were obtained with an array size of 1,600 × 1,600 pixels and 24-bit color, and 58 fundus images were obtained with an array size of 2,800 × 2,800 pixels with 24-bit color. Fifty eight fundus images were sketched by an ophthalmologist. An example of a color fundus image is shown in Fig. 1 (a).

Subsequently, the scale of the matrix was first reduced to the width 640 pixels by obtaining detailed subsamples from the original image data to improve processing efficiency.

C. Image normalization

Due to the flash light used in obtaining the fundus images, there is an atypical change in the color of the fundus images. We suggested a scheme of brightness correction using hue saturation value (HSV) space. First, the brightness values of the HSV space were calculated. The brightness correction value $Bc(i, j)$ is given by the following equation:

$$Bc(i,j)=\sqrt{1-\{V(i,j)-1\}^2} \qquad (1)$$

where $V(i, j)$ is the brightness value of the HSV space.

Next, the red value $R(i, j)$, green value $G(i, j)$, and blue value $B(i, j)$ changed by $Bc(i, j)$. The brightness was equally corrected from the center to the skirt region of the fundus image (as shown in Fig. 1 (b)). The color fundus images corrected by $Bc(i, j)$ were then processed by gamma correction. The gamma value was experimentally set to 1.5 (as shown in Fig. 1 (c)). Finally, the histograms of each red, blue, and blue-bit were extended (as shown in Fig. 1 (d)). The fundus images were standardized by using these processes.

D. Detection of optic nerve head and hemorrhage candidates

The color images were converted into grayscale images by selecting only the green component. The optic nerve head was then extracted using the p-tile thresholding method [14].

Next, the blood vessels and the hemorrhage candidates were detected by using density analysis [13]. Firstly, two smoothed images were made by using masks of 3 × 3 pixels and 9 × 9. Then, the difference in the pixel values between two smoothed images was calculated and the blood vessels and the hemorrhage candidates were detected. Finally, the blood vessel candidates connected to the optic nerve head were eliminated and the blood vessel candidates with large or very small areas were eliminated.

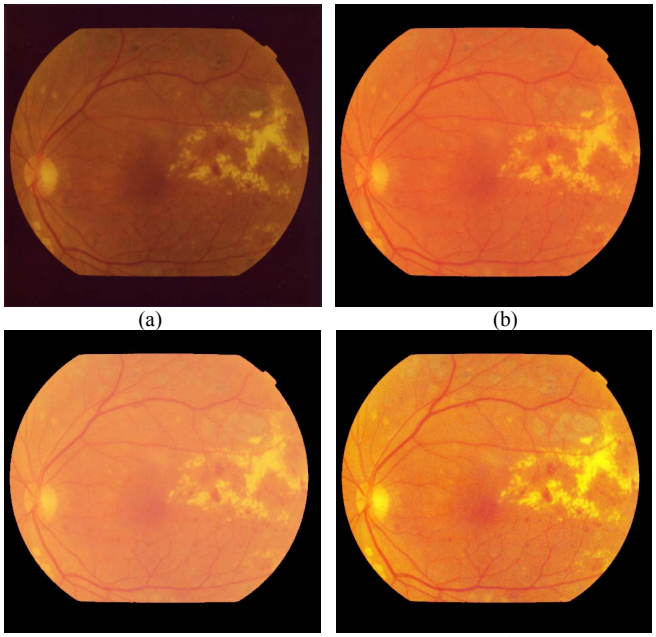

Fig. 1. Color contrast enhancement. (a) Original color fundus image. (b) Brightness of fundus image was changed by the nonlinear curve with brightness values of HSV space. (c) Image after processing by gamma correction. (d) Image was adjusted in the dynamic range.

E. Elimination of incorrectly detected blood vessels

The hemorrhage candidates were connected to the blood vessel candidates. Therefore, our method [13] could not separate the connected candidates into hemorrhage and blood vessel candidates. Firstly, the threshold value was selected in such a manner that the blood vessels could be continuously detected. The centerlines of the blood vessels were extracted by using a thinning technique. Subsequently, the centerlines with large areas were extracted in such a manner that the hemorrhage candidates could not be extracted. Finally, the blood vessels extracted with the centerlines were eliminated in order to avoid the blood vessels from being incorrectly detected.

However, all the FPs on the blood vessels were not eliminated by the method proposed in above method. Hence, the remaining FPs were eliminated by evaluating the length-to-width ratio [13]. The value of this ratio was small when the blood vessel was incorrectly detected as a candidate.

F. Elimination of false positives by feature analysis

On the original green-bit image, the minimum rectangular region that surrounds the hemorrhage candidates extends beyond five pixels in each direction along the X and Y axes was defined. The average pixel values inside and outside the hemorrhage candidate region were calculated, and the contrast was determined by evaluating the ratio between the two average values.

Furthermore, we proposed a cascade classification process. At first, the FPs were eliminated by a rule-based method using 45 features. Typical FPs were eliminated in this step.

We extracted the following 15 features from the rectangular regions: 12 features calculated from the co-occurrence matrix [15], two features based on gray-level difference statistics [16], and one feature determined by the extrema method. The 12 features from the co-occurrence matrix were (1) angular second moment, (2) contrast, (3) correlation, (4) sum of squares, (5) inverse difference moment, (6) sum average, (7) sum variance, (8) sum entropy, (9) entropy, (10) difference variance, (11) difference entropy, and (12) information measurements for correlation. The two features based on gray-level difference statistics were (13) angular second moment and (14) mean. The minimum rectangular region that surrounds the candidates was determined. These features were calculated in the rectangular regions in the three grey-level images, which comprised red, green, and blue-bit images.

Finally, the FPs were eliminated by employing using 3 Mahalanobis distance (MD) classifiers. Each classifier was trained and designed with the above 15 features obtained from 3 different gray level images separately.

III. Results and Discussions

The contrast of hemorrhages in the images was enhanced. The contrast of the processed image was higher than that of the original image. Moreover, the color of the processed image was standardized by the histogram extended method. However, if the fundus image has some laser marks, the marks are changed blighter and more obscure than the original color pixel.

A training dataset of 20 fundus images was used in setting the parameters experimentally. The images were of screen-detected DR patients and were acquired in a diagnostic examination in a municipal hospital.

A training dataset of 20 fundus images was used in setting the parameters experimentally. The images were of screen-detected DR patients and were acquired in a diagnostic examination in a municipal hospital. The sensitivity was 95% (19/20). To eliminate the incorrectly detected true hemorrhages, we used 45 calculated features. One hundred and twelve hemorrhages were detected with 630 FPs in 20 fundus images, and the threshold values of the 45 features were set experimentally to the maximum and minimum values of each 45 features on 630 FPs.

Table 1 shows the number of FPs eliminated by using the rule-based method. In Table 1, the most effective grey-scale image is the green-bit image. Moreover, the most valid feature was the information measure of correlation from the co-occurrence matrix for the green-bit image, which could eliminate 74 FPs (12%) by the rule-based method. However, four features measured on the green-bit image were not useful in eliminating any false positive. When we used 45 features for the elimination of FPs, 166 FPs (26%) were eliminated without the loss of a true positive.

Then, we constructed 3 MD classifiers; we used 45 features for each grey-scale image (as shown in Table 2). When we constructed only MD classifiers by using 112 true positives and 630 FPs, 117 FPs (19%) were eliminated. Table 2 shows that the most effective image is the blue-bit one, though Table

Table 1. The false positives were eliminated by 45 rule-based methods.

Features	*Red*	*Green*	*Blue*
Extrema	19	9	1
CM: Angular second moment	3	26	6
Contrast	25	5	12
Correlation	3	8	16
Sum of squares	24	37	7
Inverse difference moment	4	2	8
Sum average	3	3	10
Sum variance	23	0	11
Sum entropy	24	0	14
Entropy	23	7	9
Difference variance	26	0	14
Difference entropy	23	0	12
Information measurements	39	74	17
GD: Angular second moment	3	2	11
Mean	28	5	12
Subtotal	58	105	44
Total	166		

CM: co-occurrence matrix, GD: gray-level difference statistics

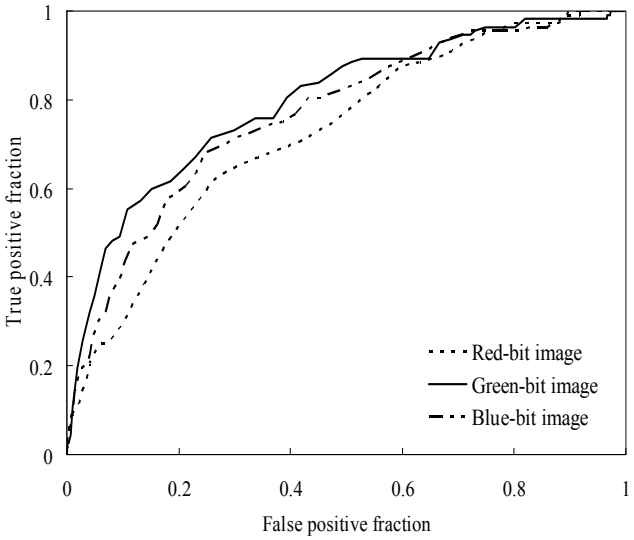

Fig. 2. ROC curves by using 3 Mahalanobis distance classifiers in training dataset.

Table 2. The false positives were eliminated by three Mahalanobis distance classifiers.

	Red	Green	Blue
MD classifier	52	17	64
Three MD classifiers combined	117		
Forty five rule-based methods and Three MD classifiers combined	219		

1 showed the most effective image was green-bit one. Moreover, three ROC curves of three MD classifiers show in Fig. 2. The false positive rate of red-bit image's MD classifiers was 0.91 in Fig. 2, when the true positive ratio was 1.0. The green ones' false positive ratio was 0.97, the blue one was 0.90. However, Fig. 2 shows that green-bit's curve was most effective in three ROC curves. If more fundus images are tested, green's curve will be demonstrated as most effective one. Subsequently, 219 FPs (35%) were eliminated using a rule-based method and three MD classifiers.

After that, to evaluate our method of detecting hemorrhages, we examined 125 fundus images; hemorrhages were detected in 35 images, and no abnormal cases were detected in the remaining 90 images. The 125 images included 38 post-screen-detected diagnostic images obtained in a municipal hospital, and 87 images were obtained in mass screening in the health academies. By using our scheme, we succeeded in obtaining satisfactory results with a sensitivity of 80% (28/35) when the specificity was 80% (72/90). And the sensitivity using our previous method was 80% when specificity was 32% (29/90). Moreover, the number of FPs per image using our previous method and new one were 1.79 and 0.26. Therefore, our proposed scheme could remove many FPs. However, our scheme could not detect approximately 20% of hemorrhages. The main reason was that hemorrhages that touched the blood vessel were undetectable. Our algorithm was not able to separate the blood vessel regions and hemorrhage regions, and therefore such hemorrhages were removed together with the blood vessels.

Finally, we measured the computation time of our method. We used an Intel Core2Duo T7400-mounted (2.16 GHz) computer with a 1.5-GB memory operating in the Windows XP Professional with the Intel C++ compiler. Processing each image required approximately 10s. There were testing fundus images on the network access server (NAS), and the file size per image was approximately 18 MB. Nagayoshi et al. detected the hemorrhages by using Matched-filtering and the color feature analysis [6]. But, Matched-filtering technique had the drawback of a long operation time. On the other hand our method using density analysis was so simple that our method could detect hemorrhages faster than previous reports.

IV. CONCLUSION

In this study, a new scheme for automatic detection of hemorrhages is presented by using digitized noncontrast fundus images as an example. This scheme can be applied to the computer-aided diagnosis (CAD) system for diagnosing eye diseases. The results of the preliminary testing showed a desirable consistency with those obtained from the proposed scheme. It was demonstrated that the algorithm detected abnormalities with high accuracy and reliability. The result of the initial work on fundus images clarified that the efficiency and accuracy of the diagnosis of DR was considerably improved. In the future, the integrated fundus image analysis scheme will be further improved and more clinical cases will be reported for evaluating its accuracy. The techniques employed in our system will help in improving diagnostic accuracy as well as in reducing the workload of ophthalmologists in the future.

REFERENCES

[1] Health and Welfare Statistics Association, *J. Health Welfare Stat.*, vol. 51, pp. 144–148, 2004.

[2] A. D. Fleming, S. Philip, K. A. Goatman, J. A. Olson, and P. F. Sharp, "Automated microaneurysm detection using local contrast normalization and local vessel detection," *IEEE Trans. Medical Imaging*, vol. 25, no. 9, pp. 1223–32, 2006.

[3] C. Serrano, B. Acha, and S. Revuelto, "2D adaptive filtering and region growing algorithm for the detection of microaneurysms," in *Proc. SPIE Medical Imaging 2007: Image Processing*, San Diego, 2004, vol. 5370, pp. 1924–1931.

[4] D. Usher, M. Dumskyj, M. Himaga, T. H. Williamson, S. Nussey, and J. F. Boyce, "Automated detection of diabetic retinopathy in digital retinal images: a tool for diabetic retinopathy screening," *Diabetic UK Diabetic Medicine*, vol. 21, no. 1, 84–90, 2004.

[5] M. Niemeijer, B. V. Ginneken, J. Staal, M. S. Suttorp-Schulten, and M. D. Abramoff, "Automatic detection of red lesions in digital color fundus photographs," *IEEE Trans. Medical Imaging*, vol. 24 no. 5, pp. 584–592, 2005.

[6] H. Nagayoshi, Y. Hiramatsu, T. Kagehiro, Y. Mizuno, M. Himaga, H. Sakou, S. Sato, H. Fukushima, and S. Kato, "Detection of lesions from fundus images for diagnosis of diabetic retinopathy," *IEICE Technical Report*, vol. 105, no. 64, pp. 61–66, 2005.

[7] E. Grisan, A. Ruggeri,"Segmentation of candidate dark lesions in fundus images," in *Proc.29th IEEE EMBS*, Lyon, France, 2007, pp. 6735-6738.

[8] Y. Hatanaka, T. Nakagawa, Y. Hayashi, A. Aoyama, X. Zhou, T. Hara, H. Fujita, Y. Mizukusa, A. Fujita, and M. Kakogawa, "Automated detection algorithm for arteriolar narrowing on fundus images," in *Proc. 27th IEEE EMBS*, Shanghai, 2005, paper#291.

[9] R. Takahashi, Y. Hatanaka, T. Nakagawa, Y. Hayashi, A. Aoyama, Y. Mizukusa, A. Fujita, M. Kakogawa, T. Hara, and H. Fujita, "Automated analysis of blood vessel intersections in retinal images for diagnosis of hypertension," *Medical Imaging Technology*, vol. 24, no. 4, pp. 270–276, 2006.

[10] Y. Hayashi, T. Nakagawa, Y. Hatanaka, A. Aoyama, Y. Mizukusa, A. Fujita, M. Kakogawa, T. Hara, H. Fujita, and T. Yamamoto, "Detection of retinal nerve fiber layer defects in retinal fundus images using Gabor filtering," in *Proc. SPIE Medical Imaging 2007: Computer-aided Diagnosis*, San Diego, vol. 6514, pp. 65142Z-1-65142Z-8.

[11] Y. Hatanaka, Y. Hayashi, T. Nakagawa, A. Aoyama, X. Zhou, T. Hara, H. Fujita, Y. Mizukusa, A. Fujita, and M. Kakogoawa, "Development of Computer-aided Diagnosis System for Fundus Images," in *8th International Conference on Medical Image Computing and Computer-assisted Intervention: Short Paper*, Palm Springs, CA, *2005,* http://www.miccai2005.org.

[12] T. Nakagawa, Y. Hayashi, Y. Hatanaka, A. Aoyama, T. Hara, A. Fujita, M. Kakogawa, H. Fujita, and T. Yamamoto, "Three-dimensional reconstruction of optic nerve head from stereo fundus images and its quantitative estimation," in *Proc. 29th IEEE Engineering in Medicine and Biology Conference Management System Annual International Conference*, Lyon, 2007, vol. 6747–6750.

[13] Y. Hatanaka, T. Nakagawa, Y. Hayash, A. Fujita, Y. Mizukusa, M. Kakogawa, K. Kawase, T. Hara, and H. Fujita, "CAD scheme for detection of hemorrhages and exudates in ocular fundus images," in *Proc. SPIE Medical Imaging 2007: Computer-aided Diagnosis*, San Diego, 2007, vol. 6514, pp. 65142M-1-65142M-8.

[14] W. Doyle, "Operation useful for similarity-invariant pattern recognition," *J. Association for Computing Machinery*, vol. 9 no. 2, pp. 259–267, 1962.

[15] R. M. Haralick, "Statistical and structural approaches to texture," *Proc. IEEE*, vol. 67, no. 5, pp. 786-804, 1979.

[16] J. S. Weszka, C. R. Dyer, and A. Rosenfeld, "A comparative study of texture measures for terrain classification," *IEEE Trans. Systems, Man, and Cybernetics*, vol. SMC-6, no. 4, pp. 269–285, 1976.